Journal of Alloys and Compounds 782 (2019) 887–892

Contents lists available at ScienceDirect

Journal of Alloys and Compounds

journal homepage: http://www.elsevier.com/locate/jalcom

A facile method to directly deposit the large-scale Ag nanoparticles on a silicon substrate for sensitive, uniform, reproducible and stable SERS substrate

Tung-Hao Chang [a, b], Yu-Cheng Chang [c, *], Chien-Ming Chen [c], Kai-Wei Chuang [c], Chia-Man Chou [d, e]

[a] Department of Radiation Oncology, Changhua Christian Hospital, Changhua, 50006, Taiwan
[b] Department of Radiological Technology, Yuanpei University, Hsinchu, 30015, Taiwan
[c] Department of Materials Science and Engineering, Feng Chia University, Taichung, 40724, Taiwan
[d] Department of Surgery, Taichung Veterans General Hospital, Taichung, 40705, Taiwan
[e] College of Medicine, National Yang-Ming University, Taipei, 11221, Taiwan

ARTICLE INFO

Article history:
Received 6 October 2018
Received in revised form
14 December 2018
Accepted 21 December 2018
Available online 22 December 2018

Keywords:
Surface-enhanced Raman scattering
Replacement reduction method
Ag nanoparticles
Reproducibility
Stability

ABSTRACT

In this study, we report a facile replacement reduction method to directly deposit the large-scale Ag nanoparticles on a silicon substrate at the room temperature and short reaction time (3 min). The reaction process is a straightforward wet chemistry approach using silver nitrate and hydrogen fluoride as a silver source and reducing reagent, respectively. The Ag nanoparticles as a surface-enhanced Raman scattering (SERS) substrate present high sensitivity, excellent uniformity, and high stability for rhodamine 6G molecules. Also, Ag nanoparticles are also shown to provide a unique platform for the SERS detection of melamine, 5-fluorouracil, amoxicillin in different aqueous media. The fabrication of Ag nanoparticles is facile, low cost, strong enhancement, low detection limit, high reproducibility, and stability, which is advantageous for the applications of other SERS-based sensors.

1. Introduction

Surface-enhanced Raman scattering (SERS) is one of the most promising analytical techniques, which has attracted scientist interest due to its high sensitivity, rapid response, unique spectroscopic fingerprint, and nondestructive data acquisition [1–3]. SERS is a powerful analytical technique that can use to detect the trace concentrations of chemical molecules or biomolecules and provides a wealth of structural information [4–6]. Due to its unique characteristics, SERS has used as a useful tool for sensing of metals ions, chemical reagents, organic pollutants, pH, DNA, proteins, nucleic acids, glucose, small or large molecules under the different environments [7–10]. Also, SERS can also be used to combine with other analytical techniques, such as liquid chromatography (LC) [11], high-performance liquid chromatography (HPLC) [12], solid phase microextraction (SPME) [13,14], and UV–vis spectroscopy [15,16].

It has demonstrated that SERS substrates play a significant role in the sensitivity and stability of SERS detection [17,18]. Recently, various approaches and techniques have been developed to fabricate highly sensitive SERS substrates [19–21]. However, the ability to create more uniform and reproducible SERS substrates is still a significant challenge. Recently, SERS substrates have mainly dominated by the absorption of analytes on rough metallic surfaces, such as gold (Au), silver (Ag), or copper (Cu) [22]. Among them, Au and Ag commonly use as SERS substrates due to their higher stability rather than Cu under ambient condition [23]. Compared to Au, Ag can provide higher SERS enhancement (10–100 times) and excite from the UV to the infrared (IR) region for the SERS applications in different fields [24–26].

There are different kinds of methods used to fabricate Ag nanostructures on the solid substrates for SERS substrates, such as thermal evaporation [27,28], ion sputtering [29], vapor-phase synthesis [30], electrochemical [31–33], self-assembly [34], wet chemical [35,36], replacement reduction [37,38], and electroless deposition methods [39]. Among them, electroless deposition is a

* Corresponding author.
E-mail address: yuchchang@fcu.edu.tw (Y.-C. Chang).

https://doi.org/10.1016/j.jallcom.2018.12.264
0925-8388/

particularly attractive method to synthesize Ag nanostructures on the silicon-based substrate by a single reaction step [39]. For electroless deposition processes, the deposition of Ag nanostructures from silver nitrate and hydrogen fluoride aqueous solution is an electrochemical redox reaction in which both anodic and cathodic processes coincide at the surface of a silicon substrate by exchanged these charges [40]. The relation of concentration of silver nitrate and hydrogen fluoride is not only used to grow random orientation of Ag dendrites on the silicon substrates but also etched silicon substrate to form silicon nanowires [41]. How to effectively grow a regular silver nanostructure on a silicon substrate has always been an important issue.

In this work, we report a one-step and straightforward process to directly deposit Ag nanoparticles on a silicon substrate with the large-scale area by replacement reduction method. The surface-enhanced Raman scattering of the silver nanoparticles was also investigated to detect rhodamine 6G, melamine, 5-fluorouracil, amoxicillin in different aqueous media. The fabrication of Ag nanoparticles is feasible, large-scale, low detection limit, high reproducibility and stability, and which shall be advantageous for other commercial applications of SERS sensing.

2. Experimental

2.1. Synthesis

Fig. 1 presents the approach for fabricating Ag nanoparticles on the silicon substrate by the replacement reduction method. This Si (001) substrate with the size of 1 cm × 1 cm was ultrasonically cleaned in ethanol and dilute hydrogen fluoride (HF) solution for 15 min and 1 min to dissolve organic contamination and native oxide layers on the surface, respectively. Ag nanoparticles were grown on the silicon substrate by a replacement reduction method in 10 mL aqueous solution containing the appropriate concentration of silver nitrate (8 mM) and hydrofluoric acid (90 mM) at room temperature for 3 min. Finally, the product substrate washed by deionized water and ethanol each, which dried with an air purge.

2.2. Characterization

The surface morphologies of Ag nanoparticles obtained by a field-emission scanning electron microscope (FESEM, Hitachi S-4800). The microstructures of Ag nanoparticles examined by field-emission transmission electron microscope (FETEM, JEOL-2100F). X-ray diffraction (XRD) measurement was carried out on a powder diffractometer (Bruker D2 phaser). The SERS spectra collected on a confocal Raman micro-spectrometer (MRI532S, Protrustech, Taiwan) with a laser wavelength of 532 nm at room temperature.

3. Results and discussion

Fig. 2a and b presents the low- and high-magnification tilt-view

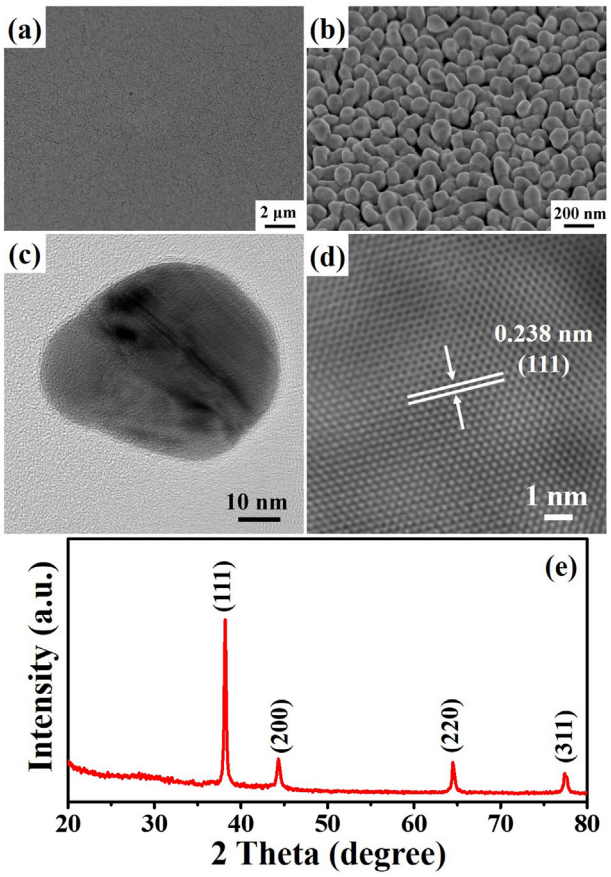

Fig. 2. The (a) low- and (b) high-magnification of SEM images of Ag nanoparticles directly grown on the silicon substrate. (c) TEM and (d) HRTEM images of an Ag nanoparticle. (e) XRD spectrum of Ag nanoparticles grown on the silicon substrate. (For interpretation of the references to colour in this figure legend, the reader is referred to the Web version of this article.)

FESEM images depicting the Ag nanoparticles are directly grown on the silicon substrate by a replacement reduction method with the reaction precursors (silver nitrate (8 mM) and hydrofluoric acid (90 mM)) at room temperature for 3 min. The Ag nanoparticles exhibited the complete and large-scale to deposit on the silicon substrate. Fig. 2c displays a FETEM image of an Ag nanoparticle with a size of 51 nm. Lattice image (Fig. 2d) shows interplanar spacing of 0.238 nm corresponds to the (111) lattice plane of cubic Ag (JCPDS Card No. 04-0783). Powder XRD was employed to verify the crystal structure and phase purity of Ag nanoparticles, as shown in Fig. 2e. It can see that the four diffraction peaks at the 2θ positions 38.1°, 44.3°, 64.5°, and 77.4° correspond to the (111), (200), (220), and (311) planes of cubic Ag (JCPDS Card No. 04-0783). Also, no significant diffraction peaks arising from crystalline impurities can be

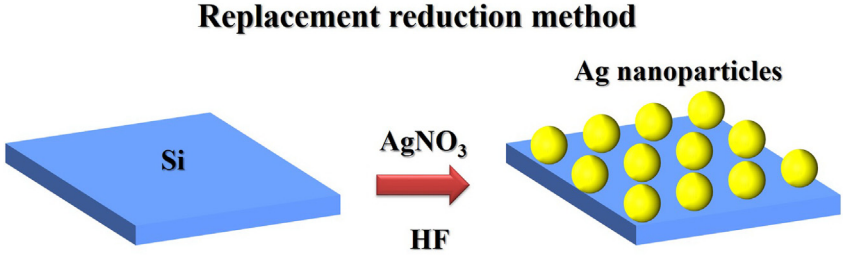

Fig. 1. Schematic diagram for the fabrication of Ag nanoparticles by a replacement reduction method.

detected, indicating that the product is a pure cubic Ag phase.

To investigate the performance of Ag nanoparticles in the SERS detection, rhodamine 6G (R6G) can select as a probe molecule. This silicon substrate with Ag nanoparticles (Fig. 2a) was immersed in deionized water of R6G (10^{-6} M) for 1 h and then rinsed with deionized water to remove the unbound molecules. After dried under an air purge, we randomly detected the SERS spectra of the R6G with the same concentration from 5 spots under the same laser power, as shown in Fig. 3a. The primary vibration peaks of R6G are 1185 (in-plane vibration of C—H bonds), 1311 (C—C stretching), 1360 (aromatic C—C stretching vibration mode), 1507 (aromatic C—C stretching vibration mode), and 1645 (aromatic C—C stretching vibration mode) cm^{-1} [25]. The position and intensity of the Raman peak do not show a significant change, and the intensity of all peaks is within 9% variation range for the 5 spots. This result demonstrates that Ag nanoparticles with high homogeneity. The reproducibility of the SERS substrate is one of the essential parameters for SERS applications. In this study, the recycling ability of the Ag nanoparticles can obtain from the same substrate before and after irradiated with UV lamp over three cycles, as shown in Fig. 3b. For each cycle, this substrate could be entirely photodegraded by irradiated 36 W UV lamp (max. 350 nm, PL-L, Philip) for 1 h. This substrate immersed in a fresh R6G solution (10^{-6} M) for another cycle of SERS measurement. The photodegraded mechanism of R6G may ascribe to Ag nanoparticles photoexcited to facilitate the generation of electrons and Ag^{+} (h^{+}) ions by surface plasmon resonance under UV-light irradiation. Due to the Ag^{+} (h^{+}) ions are also reactive radical species, which can also directly oxidize R6G and reduce to metallic Ag again [42,43]. This result indicates that Ag nanoparticles can maintain a relatively high SERS enhancement even after three cycles.

The SERS detection limit of the Ag nanoparticles can determine by immersing R6G solutions of different concentrations 10^{-8} to 10^{-10} M, as shown in Fig. 4a. The main SERS peaks of R6G gradually increased with increasing the concentration of the R6G solution. Due to the SERS peak at 1645 cm^{-1} does not overlap with other peaks, which selects as the marker peak of R6G. The intensity of the R6G Raman signal achieved at the critical concentration of 10^{-10} M, which revealed the SERS detection limit of Ag nanoparticles for the detection of the R6G solution. To demonstrate that Ag nanoparticles can also apply to detect R6G in different aqueous media. Herein, we used three kinds of aqueous media to dissolve R6G molecules for the SERS measurement, as shown in Fig. 4b. The three types of aqueous media are deionized water, reverse osmosis water, and tap water, respectively. Even if the R6G molecule was dissolved in tap water or reverse osmosis water, the Raman signal did not exhibit any significant change. The results demonstrate that Ag nanoparticle can also use to detect R6G molecules under the more complex matrix of water.

To demonstrate that Ag nanoparticles can use for the detection of different kinds of toxic chemical. Herein, we investigated the SERS properties of Ag nanoparticles using melamine as a probe molecule. Melamine is a toxic chemical and nitrogen-rich compound, which mainly applies in the production of flame retardants, commercial filters, and kitchenware, etc. Its widespread use may result in trace amounts of melamine in food [44,45]. Fig. 5a shows

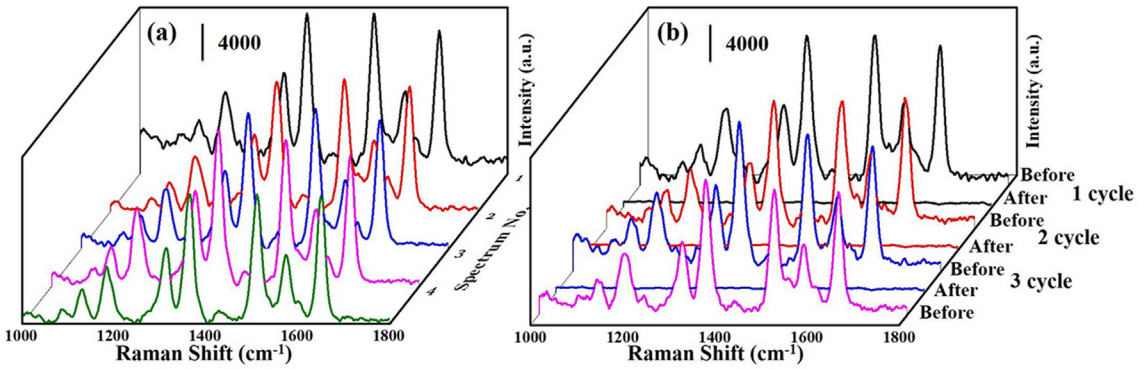

Fig. 3. (a) The SERS spectra of the R6G (10^{-6} M) from 5 randomly selected spots on the silicon substrate with Ag nanoparticles. (b) The SERS spectra of R6G (10^{-6} M) before and after the irradiation of UV light in 3 cycles on the silicon substrate with Ag nanoparticles. (For interpretation of the references to colour in this figure legend, the reader is referred to the Web version of this article.)

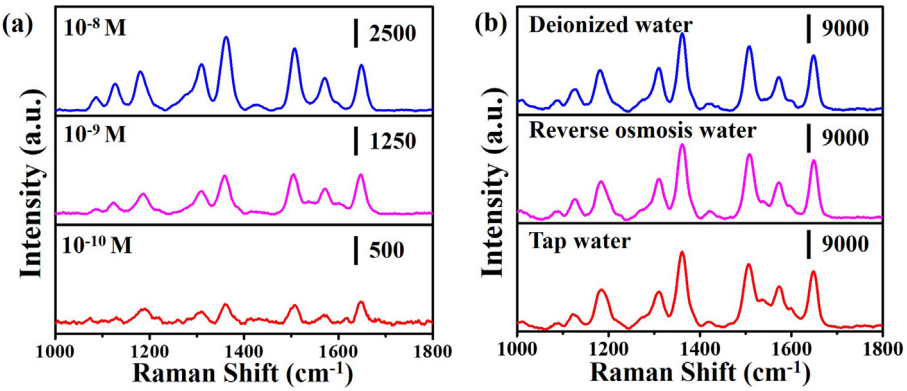

Fig. 4. The SERS spectra of the different concentrations of R6G adsorbed on the silicon substrate with Ag nanoparticles from 10^{-8} to 10^{-10} M. (b) The SERS spectra of the R6G (10^{-6} M) dispersed in different aqueous media. (For interpretation of the references to colour in this figure legend, the reader is referred to the Web version of this article.)

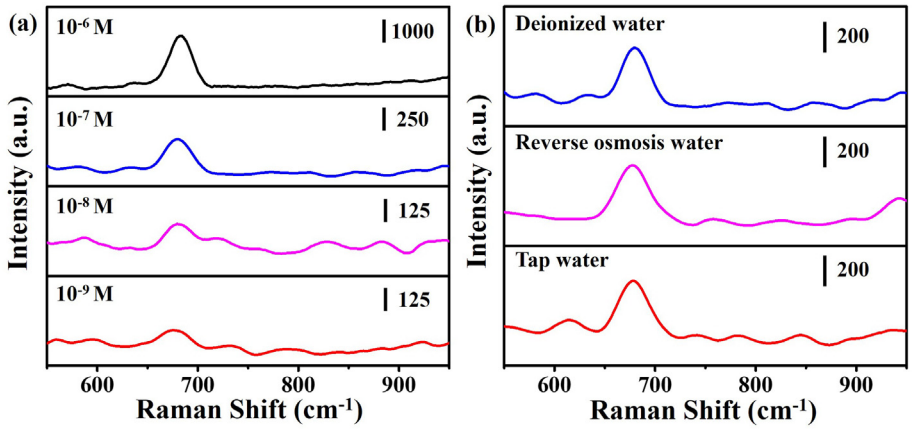

Fig. 5. (a) The SERS spectra of the different concentrations of melamine absorbed on the silicon substrate with Ag nanoparticles from 10^{-6} to 10^{-9} M. (b) The SERS spectra of the melamine (10^{-7} M) dispersed in different aqueous media. (For interpretation of the references to colour in this figure legend, the reader is referred to the Web version of this article.)

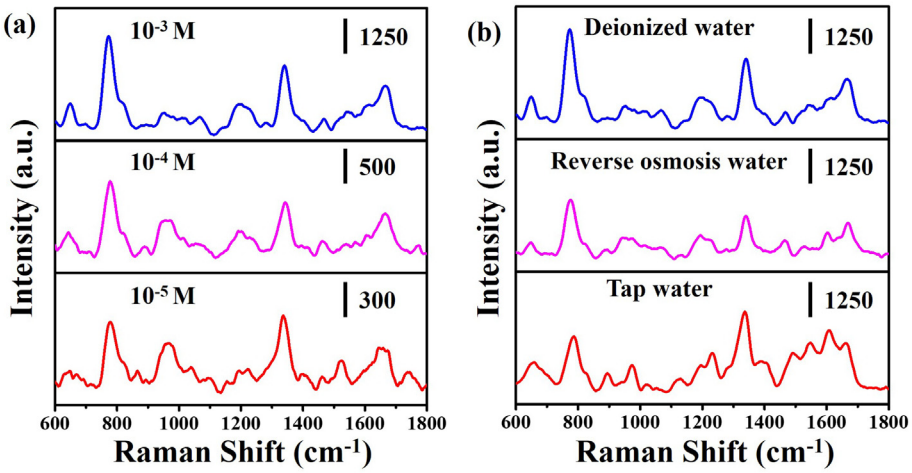

Fig. 6. (a) The SERS spectra of the different concentrations of 5-fluorouracil absorbed on the silicon substrate with Ag nanoparticles from 10^{-3} to 10^{-5} M. (b) The SERS spectra of the 5-fluorouracil (10^{-3} M) dispersed in different aqueous media. (For interpretation of the references to colour in this figure legend, the reader is referred to the Web version of this article.)

the SERS spectra obtained when immersed in melamine solutions of different concentrations, following the same procedure from low to high concentration (10^{-6} to 10^{-9} M) as that in the R6G measurements. Even if the concentration of the melamine solution is down to 10^{-9}, the Raman peak at 682 cm^{-1} can clearly observe. Also, melamine molecules (10^{-7} M) were also dissolved in the three types of aqueous media for the SERS measurement, as shown in Fig. 5b. The results show that there was no noticeable change in the intensity and position of the Raman signal.

To further prove that the Ag nanoparticles can also apply to the detection of drugs. Herein, we adopt two different kinds of drugs for the SERS measurement. The two different types of medicines are 5-fluorouracil (5-FU) and amoxicillin, respectively. 5-FU is an antimetabolite of the pyrimidine analog type and a well-known anticancer drug widely used in the treatment of solid cancers, such as stomach, colon, lung, and breast cancers [46,47]. Amoxicillin is an antibacterial drug and widely used to treat bacterial infections in humans and animals [48,49]. For the detection of 5-FU, the SERS spectra obtained with the different concentrations (10^{-3} to 10^{-5} M) of 5-FU on the Ag nanoparticles, as shown in Fig. 6a. In this case, the detection concentration of 5-FU is as lower as 10^{-5} M, which is lower than the value (1.5×10^{-5} M) of the detected concentration for the previous report [50]. For the different aqueous media, the intensity of the Raman signal for 5-FU dissolved in tap water or reverse osmosis water exhibited evidence decrease rather than 5-FU dissolved in deionized water, as shown in Fig. 6b. This phenomenon shall ascribe to tap water or reverse osmosis water contain trace amounts of chloramine that can react with the N–H bond to form N–Cl bond in the pyrimidine ring of 5-FU and affect the measurement of the Raman signal. In the previous work, the chloramine may transfer their active chlorine to other amine groups (such as amines, amino acids, peptides, etc.) [51]. For the detection of amoxicillin, the SERS spectra obtained with the different concentrations (10^{-5} to 10^{-8} M) of amoxicillin on the Ag nanoparticles, as shown in Fig. 7a. The distinct characteristic peaks observed even when the amoxicillin concentration was down to 10^{-8} M. Also, amoxicillin molecules (10^{-3} M) were also dissolved in the three types of aqueous media for the SERS measurement (Fig. 7b), which was also no apparent change in the intensity and position of Raman signal. The results indicate that Ag nanoparticles would potentially apply to the trace detection of persistent toxic chemicals and drugs in different aqueous media.

4. Conclusions

Large-scale and high-density Ag nanoparticles have directly

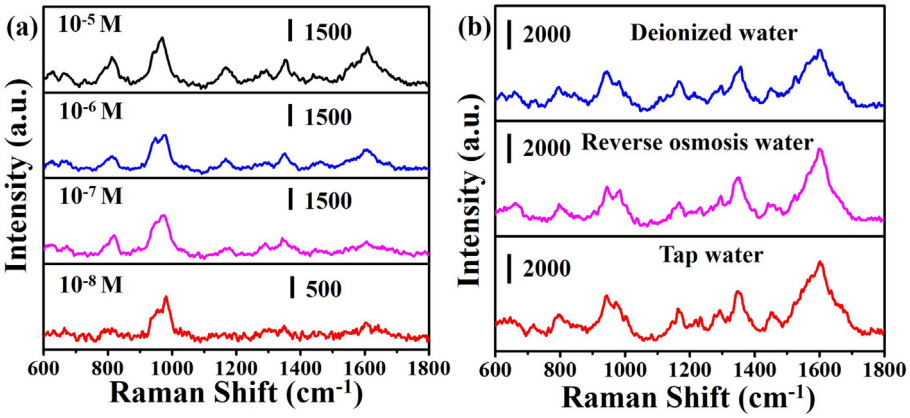

Fig. 7. (a) The SERS spectra of the different concentrations of amoxicillin absorbed on the silicon substrate with Ag nanoparticles from 10^{-5} to 10^{-8} M. (b) The SERS spectra of the amoxicillin (10^{-3} M) dispersed in different aqueous media. (For interpretation of the references to colour in this figure legend, the reader is referred to the Web version of this article.)

grown on a silicon substrate by using a replacement reduction method at the room temperature. The silver nanoparticles can provide an excellent platform for SERS, yielding detection levels for R6G (10^{-10} M), melamine (10^{-9} M), 5-fluorouracil (10^{-5} M), and amoxicillin (10^{-8} M), respectively. The Ag nanoparticles provide simplicity, high reproducibility, high enhancement, low detection limits, and low-cost manufacturing, which are of great value for the practical application of other SERS sensing systems.

Acknowledgments

This study was supported financially by the Ministry of Science and Technology of Taiwan (MOST 106-2221-E-035-032-MY3 and MOST 107-2218-E-035-010-) and Taichung Veterans General Hospital (TCVGH-1075401C and TCVGH-FCU1078204). The authors appreciate the Precision Instrument Support Center of Feng Chia University in providing the fabrication and measurement facilities.

References

[1] W.P. Ambrose, P.M. Goodwin, J.C. Martin, R.A. Keller, Single molecule detection and photochemistry on a surface using near-field optical excitation, Phys. Rev. Lett. 72 (1994) 160–163.
[2] L. Yang, P. Li, J. Liu, Progress in multifunctional surface-enhanced Raman scattering substrate for detection, RSC Adv. 4 (2014) 49635–49646.
[3] J. Li, Z. Zhu, B. Zhu, Y. Ma, B. Lin, R. Liu, Y. Song, H. Lin, S. Tu, C. Yang, Surface-enhanced Raman scattering active plasmonic nanoparticles with ultrasmall interior nanogap for multiplex quantitative detection and cancer cell imaging, Anal. Chem. 88 (2016) 7828–7836.
[4] F.-H. Ko, M.R. Tai, F.-K. Liu, Y.-C. Chang, Au–Ag core–shell nanoparticles with controllable shell thicknesses for the detection of adenosine by surface enhanced Raman scattering, Sensor. Actuator. B Chem. 211 (2015) 283–289.
[5] F.-H. Ko, Y.-C. Chang, Aptamer based surface enhanced Raman scattering detection of adenosine using various core sizes of Au-Ag core-shell nanoparticles, RSC Adv. 4 (2014) 26251–26257.
[6] M. Shaban, A.R. Galaly, Highly sensitive and selective in-situ SERS detection of Pb2+, Hg2+, and Cd2+ using nanoporous membrane functionalized with CNTs, Sci. Rep. 6 (2016) 25307.
[7] J. Ni, R.J. Lipert, G.B. Dawson, M.D. Porter, Immunoassay readout method using extrinsic Raman labels adsorbed on immunogold colloids, Anal. Chem. 71 (1999) 4903–4908.
[8] L. Fabris, M. Dante, G. Braun, S.J. Lee, N.O. Reich, M. Moskovits, T.-Q. Nguyen, G.C. Bazan, A heterogeneous PNA-based SERS method for DNA detection, J. Am. Chem. Soc. 129 (2007) 6086–6087.
[9] Y. Wang, J. Irudayaraj, A SERS DNAzyme biosensor for lead ion detection, Chem. Commun. 47 (2011) 4394–4396.
[10] J.-W. Chen, X.-P. Liu, K.-J. Feng, Y. Liang, J.-H. Jiang, G.-L. Shen, R.-Q. Yu, Detection of adenosine using surface-enhanced Raman scattering based on structure-switching signaling aptamer, Biosens. Bioelectron. 24 (2008) 66–71.
[11] A. Subaihi, D.K. Trivedi, K.A. Hollywood, J. Bluett, Y. Xu, H. Muhamadali, D.I. Ellis, R. Goodacre, Quantitative online liquid chromatography–surface-enhanced Raman scattering (LC-SERS) of methotrexate and its major metabolites, Anal. Chem. 89 (2017) 6702–6709.
[12] W.A. Hassanain, E.L. Izake, A. Sivanesan, G.A. Ayoko, Towards interference free HPLC-SERS for the trace analysis of drug metabolites in biological fluids, J. Pharmaceut. Biomed. Anal. 136 (2017) 38–43.
[13] B. Li, Y.-e. Shi, J. Cui, Z. Liu, X. Zhang, J. Zhan, Au-coated ZnO nanorods on stainless steel fiber for self-cleaning solid phase microextraction-surface enhanced Raman spectroscopy, Anal. Chim. Acta 923 (2016) 66–73.
[14] C. Liu, X. Zhang, L. Li, J. Cui, Y.-e. Shi, L. Wang, J. Zhan, Silver nanoparticle aggregates on metal fibers for solid phase microextraction-surface enhanced Raman spectroscopy detection of polycyclic aromatic hydrocarbons, Analyst 140 (2015) 4668–4675.
[15] M.M.B. Pessôa, G.F.S. Andrade, M.R. dos Santos, M.L.A. Temperini, The electrochemical reduction of 2-formylpyridine thiosemicarbazone monitored by SERS and UV–vis spectroscopies, J. Electroanal. Chem. 545 (2003) 117–122.
[16] D. Saviello, M. Trabace, A. Alyami, A. Mirabile, R. Giorgi, P. Baglioni, D. Iacopino, A combined Surface Enhanced Raman Spectroscopy (SERS)/UV–vis approach for the investigation of dye content in commercial felt tip pens inks, Talanta 181 (2018) 448–453.
[17] M. Rycenga, C.M. Cobley, J. Zeng, W. Li, C.H. Moran, Q. Zhang, D. Qin, Y. Xia, Controlling the synthesis and assembly of silver nanostructures for plasmonic applications, Chem. Rev. 111 (2011) 3669–3712.
[18] M. Fan, G.F.S. Andrade, A.G. Brolo, A review on the fabrication of substrates for surface enhanced Raman spectroscopy and their applications in analytical chemistry, Anal. Chim. Acta 693 (2011) 7–25.
[19] B. Sharma, R.R. Frontiera, A.-I. Henry, E. Ringe, R.P. Van Duyne, SERS: materials, applications, and the future, Mater. Today 15 (2012) 16–25.
[20] A. Gutes, C. Carraro, R. Maboudian, Silver nanodesert rose as a substrate for surface-enhanced Raman spectroscopy, ACS Appl. Mater. Interfaces 1 (2009) 2551–2555.
[21] J. Huang, F. Chen, Q. Zhang, Y. Zhan, D. Ma, K. Xu, Y. Zhao, 3D silver nanoparticles decorated zinc oxide/silicon heterostructured nanomace arrays as high-performance surface-enhanced Raman scattering substrates, ACS Appl. Mater. Interfaces 7 (2015) 5725–5735.
[22] H. Ilkhani, T. Hughes, J. Li, C.J. Zhong, M. Hepel, Nanostructured SERS-electrochemical biosensors for testing of anticancer drug interactions with DNA, Biosens. Bioelectron. 80 (2016) 257–264.
[23] M. Fan, G.F.S. Andrade, A.G. Brolo, A review on the fabrication of substrates for surface enhanced Raman spectroscopy and their applications in analytical chemistry, Anal. Chim. Acta 693 (2011) 7–25.
[24] R. Stiufiuc, C. Iacovita, C.M. Lucaciu, G. Stiufiuc, A.G. Dutu, C. Braescu, N. Leopold, SERS-active silver colloids prepared by reduction of silver nitrate with short-chain polyethylene glycol, Nanoscale Res. Lett. 8 (2013), 47-47.
[25] H. Zhang, J. Wang, G. Li, L. Chen, H. Wang, X. Tian, Fabrication of Ag-nanosheet-assembled hollow tubular array and their SERS effect, J. Alloys Compd. 772 (2019) 663–668.
[26] H. Wang, K.B. Li, C. Xu, S.C. Xu, G.H. Li, Large-scale solvothermal synthesis of Ag nanocubes with high SERS activity, J. Alloys Compd. 772 (2019) 150–156.
[27] M.-K. Oh, Y.-S. Shin, C.-L. Lee, R. De, H. Kang, N.E. Yu, B.H. Kim, J.H. Kim, J.-K. Yang, Morphological and SERS properties of silver nanorod array films fabricated by oblique thermal evaporation at various substrate temperatures, Nanoscale Res. Lett. 10 (2015) 259.
[28] X. Zhang, S. Xu, S. Jiang, J. Wang, J. Wei, S. Xu, S. Gao, H. Liu, H. Qiu, Z. Li, H. Liu, Z. Li, H. Li, Growth graphene on silver–copper nanoparticles by chemical vapor deposition for high-performance surface-enhanced Raman scattering, Appl. Surf. Sci. 353 (2015) 63–70.
[29] Y.-C. Chang, Low temperature and large-scale growth of ZnO nanoneedle arrays with enhanced optical and surface-enhanced Raman scattering properties, Sensor. Actuator. B Chem. 225 (2016) 498–503.

[30] P. Mohanty, I. Yoon, T. Kang, K. Seo, K.S.K. Varadwaj, W. Choi, Q.H. Park, J.P. Ahn, Y.D. Suh, H. Ihee, B. Kim, Simple vapor-phase synthesis of single-crystalline Ag nanowires and single-nanowire surface-enhanced Raman scattering, J. Am. Chem. Soc. 129 (2007) 9576–9577.
[31] A. Sivanesan, E. Witkowska, W. Adamkiewicz, L. Dziewit, A. Kaminska, J. Waluk, Nanostructured silver-gold bimetallic SERS substrates for selective identification of bacteria in human blood, Analyst 139 (2014) 1037–1043.
[32] Y. Xia, Y. Wu, T. Hang, J. Chang, M. Li, Electrodeposition of high density silver nanosheets with controllable morphologies served as effective and reproducible SERS substrates, Langmuir 32 (2016) 3385–3392.
[33] C. Zhu, G. Meng, Q. Huang, Z. Zhang, Q. Xu, G. Liu, Z. Huang, Z. Chu, Ag nanosheet-assembled micro-hemispheres as effective SERS substrates, Chem. Commun. 47 (2011) 2709–2711.
[34] Q. Zhang, Y.H. Lee, I.Y. Phang, C.K. Lee, X.Y. Ling, Hierarchical 3D SERS substrates fabricated by integrating photolithographic microstructures and self-assembly of silver nanoparticles, Small 10 (2014) 2703–2711.
[35] C. Tian, Y. Deng, D. Zhao, J. Fang, Plasmonic silver supercrystals with ultrasmall nanogaps for ultrasensitive SERS-based molecule detection, Adv. Opt. Mater. 3 (2015) 404–411.
[36] N.S. Yurova, N.E. Markina, M.V. Pozharov, A.M. Zakharevich, T.Y. Rusanova, A.V. Markin, SERS-active sorbent based on aluminum oxide loaded with silver nanoparticles, Colloids Surf. A Physicochem. Eng. Asp. 495 (2016) 169–175.
[37] Y. Zhang, S. Sun, X. Zhang, L. Tang, X. Song, Z. Yang, Sulfate-ion-assisted galvanic replacement tuning of silver dendrites to highly branched chains for effective SERS, Phys. Chem. Chem. Phys. 16 (2014) 18918–18925.
[38] Y. Yang, J. Liu, Z.-W. Fu, D. Qin, Galvanic replacement-free deposition of Au on Ag for core–shell nanocubes with enhanced chemical stability and SERS activity, J. Am. Chem. Soc. 136 (2014) 8153–8156.
[39] E. Galopin, J. Barbillat, Y. Coffinier, S. Szunerits, G. Patriarche, R. Boukherroub, Silicon nanowires coated with silver nanostructures as ultrasensitive interfaces for surface-enhanced Raman spectroscopy, ACS Appl. Mater. Interfaces 1 (2009) 1396–1403.
[40] Z. Huang, N. Geyer, P. Werner, J. de Boor, U. Gösele, Metal-Assisted chemical etching of silicon: a review, Adv. Mater. 23 (2011) 285–308.
[41] K. Peng, Y. Yan, S. Gao, J. Zhu, Dendrite-Assisted growth of silicon nanowires in electroless metal deposition, Adv. Funct. Mater. 13 (2003) 127–132.
[42] L. Liang, Y. Meng, L. Shi, J. Ma, J. Sun, Enhanced photocatalytic performance of novel visible light-driven Ag–TiO2/SBA-15 photocatalyst, Superlattice. Microst. 73 (2014) 60–70.
[43] P. Christopher, H. Xin, S. Linic, Visible-light-enhanced catalytic oxidation reactions on plasmonic silver nanostructures, Nat. Chem. 3 (2011) 467.
[44] J.F. Betz, Y. Cheng, G.W. Rubloff, Direct SERS detection of contaminants in a complex mixture: rapid, single step screening for melamine in liquid infant formula, Analyst 137 (2012) 826–828.
[45] A. Kim, S.J. Barcelo, R.S. Williams, Z. Li, Melamine sensing in milk products by using surface enhanced Raman scattering, Anal. Chem. 84 (2012) 9303–9309.
[46] Y. Abdel-Mottaleb, M.S.A. Abdel-Mottaleb, Molecular modeling studies of some uracil and new deoxyuridine derivatives, J. Chem. 2016 (2016) 12.
[47] C.O. Ehi-Eromosele, B.I. Ita, E.E.J. Iweala, Silica coated LSMO magnetic nanoparticles for the pH-Responsive delivery of 5-Fluorouracil anticancer drug, Colloids Surf. A Physicochem. Eng. Asp. 530 (2017) 164–171.
[48] S. Cui, Z. Dai, Q. Tian, J. Liu, X. Xiao, C. Jiang, W. Wu, V.A.L. Roy, Wetting properties and SERS applications of ZnO/Ag nanowire arrays patterned by a screen printing method, J. Mater. Chem. C 4 (2016) 6371–6379.
[49] A. Bebu, L. Szabó, N. Leopold, C. Berindean, L. David, IR, Raman, SERS and DFT study of amoxicillin, J. Mol. Struct. 993 (2011) 52–56.
[50] Y. Xing, H. Fuss, J. Lademann, M.D. Huang, H. Becker-Ross, S. Florek, A. Patzelt, M.C. Meinke, S. Jung, N. Esser, A new concept of efficient therapeutic drug monitoring using the high-resolution continuum source absorption spectrometry and the surface enhanced Raman spectroscopy, Spectrochim. Acta B At. Spectrosc. 142 (2018) 91–96.
[51] M.P. Snyder, D.W. Margerum, Kinetics of chlorine transfer from chloramine to amines, amino acids, and peptides, Inorg. Chem. 21 (1982) 2545–2550.